

Variational Autoencoders: A Deep Probabilistic Framework for Latent Variable Modelling and Generative Inference

NAME: SIDHU NAYAK KATRAVATH

STUDENT ID: 24086840

GITHUB LINK: <https://github.com/sidhukatravath/Machine-Learning.git>

Abstract

This lesson offers a comprehensive examination of Variational Autoencoders (VAEs), a probabilistic generative model that combines deep learning with variational inference. The emphasis is on comprehending how Variational Autoencoders (VAEs) acquire latent variable distributions, optimize the evidence lower bound (ELBO), and produce coherent samples using the reparameterization method. Utilizing the MNIST dataset, we develop a Variational Autoencoder (VAE) from foundational principles, evaluate the quality of reconstruction, analyze the structure of the latent space, and measure generative efficacy. Training curves, reconstructions, and latent-space visualizations are employed to elucidate theoretical concepts like as KL regularization and continuous latent manifolds. The lesson seeks to offer both intuitive and quantitative understanding, allowing practitioners to utilize VAEs in representation learning, synthesis, and probabilistic modeling problems.

1. Preface

Variational Autoencoders (VAEs) represent a category of deep generative models that integrate neural networks with probabilistic latent variable modeling. In contrast to standard autoencoders that encode data into deterministic codes, Variational Autoencoders (VAEs) develop a comprehensive probability distribution over latent representations. This facilitates sampling, interpolation, and the creation of unique data, establishing VAEs as essential instruments in contemporary generative modeling. Their methodology is based on variational inference, aiming to create an estimated posterior for latent variables by maximizing the evidence lower bound (ELBO). This establishes a direct link between Variational Autoencoders (VAEs) and Bayesian learning, while preserving the scalability of deep neural networks.

This lesson emphasizes the fundamental mechanisms enabling Variational Autoencoders (VAEs) to acquire expressive latent spaces: the encoder functioning as an inference model, the decoder serving as a generative likelihood, and the KL divergence term that regularizes the latent distribution. Utilizing the MNIST dataset, we develop a Variational Autoencoder (VAE) from

foundational principles, visualize its latent geometry, assess reconstruction efficacy, and examine its generative characteristics. The lesson seeks to elucidate the functioning of VAEs by integrating mathematical exposition with actual experimentation, highlighting the benefits of probabilistic latent modeling over deterministic encoding.

2. Theoretical Framework

2.1 Examination of Variational Autoencoders

Variational Autoencoders (VAEs) are part of the larger category of latent variable models, wherein observations x are presumed to be derived from unobserved continuous variables z . A Variational Autoencoder (VAE) comprises two neural components: an encoder that translates data into parameters of a latent distribution, and a decoder that reconstructs data from latent samples. Training is accomplished by variational inference, which presents an estimated posterior distribution $q_\phi(z | x)$ to substitute the intractable true posterior $p(z | x)$. By optimizing the evidence lower bound (ELBO), the model concurrently promotes precise reconstruction of the input and regularizes the latent space via a KL divergence penalty. The reparameterization approach facilitates fast gradient-based optimization by permitting random sampling while preserving differentiability via the latent pathway.

2.2 Advantages and Disadvantages

Variational Autoencoders have numerous benefits compared to deterministic autoencoders. They acquire seamless, continuous latent manifolds that facilitate interpolation, controllable sampling, and generative modeling. The probabilistic latent representation promotes generalization and mitigates overfitting by regulating the latent distribution. Moreover, VAEs inherently accommodate big datasets and can be modified for many architectures, including convolutional, hierarchical, and conditional forms.

Nonetheless, VAEs demonstrate certain constraints. The Gaussian probability assumption frequently leads to indistinct reconstructions, especially with high-resolution picture data. The KL regularization term may diminish to nearly zero, resulting in latent dimensions becoming inactive—a phenomenon referred to as posterior collapse. Furthermore, the generative samples may exhibit diminished sharpness in comparison to those generated by adversarial models like GANs. Notwithstanding these issues, VAEs continue to be advantageous for applications necessitating organized latent representations rather than photorealistic production.

2.3 Previous Literature

Variational Autoencoders (VAEs) were introduced by Kingma and Welling in 2014, who developed the Evidence Lower Bound (ELBO) and the reparameterization method that constitute the foundation of contemporary implementations. Rezende et al. (2014) augmented the system by investigating stochastic backpropagation and more profound generative models. Subsequent investigations have examined enhancements in generative quality (e.g., β -VAE, InfoVAE), tackled posterior collapse, and integrated VAEs with normalizing flows to augment expressiveness. These advancements underscore VAEs as a fundamental method connecting Bayesian modeling with contemporary deep learning.

3. Mathematical Principles

Variational Autoencoders are based on latent variable modeling, wherein data x is presumed to originate from latent variables z via a generative process delineated by a prior $p(z)$ and likelihood $p_\theta(x | z)$. The objective is to optimize the marginal likelihood.

$$p_\theta(x) = \int p_\theta(x | z) p(z) dz$$

However, this integral is intractable for deep generative models. Variational Autoencoders (VAEs) optimize the Evidence Lower Bound (ELBO) by incorporating an approximate posterior $q_\phi(z | x)$:

$$\log p_\theta(x) \geq \mathbb{E}_{q_\phi(z|x)}[\log p_\theta(x|z)] - D_{\text{KL}}(q_\phi(z|x) \parallel p(z))$$

The initial term promotes precise reconstruction, but the KL divergence regularizes the latent distribution by constraining $q_\phi(z | x)$ approaches the prior, generally a standard Gaussian distribution.

To optimize this goal via gradient descent, the model must backpropagate through samples from $q_\phi(z | x)$. VAEs do this through the reparameterization trick, which reformulates sampling as:

$$z = \mu_\phi(x) + \sigma_\phi(x) \epsilon, \epsilon \sim \mathcal{N}(0, I)$$

This articulates z as a deterministic function of x and noise ϵ , rendering the stochastic trajectory differentiable concerning ϕ .

The KL term of the ELBO is analytically manageable for Gaussian posteriors:

$$D_{\text{KL}}(q_{\phi}(z | x) \parallel p(z)) = \frac{1}{2} \sum_i (\mu_i^2 + \sigma_i^2 - \log \sigma_i^2 - 1)$$

Collectively, these elements characterize a probabilistic autoencoder designed to acquire a continuous, structured latent representation of data while facilitating generative sampling from the acquired model.

4. Description of the Dataset

This course employs the MNIST handwritten digits dataset, a commonly utilized benchmark for assessing generative models. MNIST comprises 60,000 training images and 10,000 test images, each featuring a 28×28 grayscale digit ranging from 0 to 9. The dataset is ideally suited for Variational Autoencoders, since the images are both basic and sufficiently diversified to uncover significant latent structures, facilitating clear visualization of clusters and generative behavior. Each image is normalized to the range [0, 1] and flattened for input into the fully connected encoder and decoder networks. No more preprocessing is necessary. The equitable class distribution guarantees that digit categories are uniformly represented in the latent space, hence enhancing the analysis of clustering, interpolation, and reconstruction quality. The utilization of MNIST enables the lesson to concentrate on the behavior of the VAE instead of the intricacies of the dataset.

5. Implementation & Experiments

5.1 Experimental Configuration

The Variational Autoencoder was executed in PyTorch utilizing a fully connected architecture appropriate for the MNIST dataset. All photos were normalized to the range [0, 1] and converted into 784-dimensional vectors prior to being input into the encoder. The encoder has a hidden layer of 400 units, succeeded by two linear layers that generate the mean and log-variance of a two-dimensional latent variable. The decoder reflects this architecture, translating latent samples back to the 784-dimensional picture space through a sigmoid output layer. Training was conducted for 10 epochs with the Adam optimizer with a learning rate of 1×10^{-3} and a batch size of 128. A GPU was utilized when accessible to minimize training duration.

The loss function is equivalent to the negative evidence lower bound (ELBO), which is divided into a reconstruction component and a KL divergence component. The reconstruction loss is calculated using binary cross-entropy, but the KL term has a closed-form calculation owing to the presupposed Gaussian approximate posterior. Recording both components in conjunction with the total loss facilitates a comprehensive examination of training behavior.

5.2 Training Conduct

The model's performance during training was assessed by documenting the average total loss, reconstruction loss, and KL divergence per data point at the conclusion of each epoch. The values are summarized in Table 1. The overall loss exhibits a steady decline throughout the epochs, indicating enhancements in both reconstruction quality and latent space regularization. The reconstruction term diminishes consistently, signifying that the decoder increasingly excels at modeling pixel intensities. Concurrently, the KL divergence incrementally rises during the epochs, indicating that the approximate posterior increasingly aligns with the prior distribution as training advances.

Table 1. Training Loss Components per Epoch

| Epoch | Total Loss | Reconstruction Loss | KL Divergence |
|-------|------------|---------------------|---------------|
| 1 | 191.3637 | 185.5242 | 5.8395 |
| 2 | 168.4115 | 162.9912 | 5.4203 |
| 3 | 163.7463 | 158.2058 | 5.5406 |
| 4 | 161.1101 | 155.5063 | 5.6038 |
| 5 | 159.3406 | 153.6565 | 5.684 |
| 6 | 157.9629 | 152.2359 | 5.727 |
| 7 | 156.8715 | 151.0691 | 5.8024 |
| 8 | 155.989 | 150.1512 | 5.8378 |
| 9 | 155.2216 | 149.3451 | 5.8765 |
| 10 | 154.5172 | 148.5941 | 5.9231 |

5.3 Reconstruction and Latent Space Examination

Post-training, the VAE underwent qualitative assessment using the reconstruction of test images and the visualization of the latent space. Figure 1 illustrates original and rebuilt digits, indicating that the model maintains digit identity despite refining local features. Figure 2 illustrates the two-dimensional latent space, with each point representing the encoder's mean for a test image, differentiated by digit label color. The obtained clusters indicate that the VAE acquires a structured latent manifold with significant organization.

5.4 Generative Sampling

To evaluate generating performance, random samples were extracted from the standard normal prior and translated into pictures. Figure 3 illustrates that the model generates coherent digit-like samples, demonstrating that the learned latent space is well aligned with the prior to provide meaningful production.

6. Outcomes and Analysis

This section assesses the Variational Autoencoder's performance using quantitative loss measures, qualitative reconstruction quality, latent space organization, and generative sampling behavior. Collectively, these findings demonstrate the model's proficiency in acquiring a continuous and regularized latent representation of MNIST digits.

6.1 Quantitative Assessment

Table 1 encapsulates the training losses throughout epochs, whereas Figure 1 illustrate the associated training curves. The overall loss diminishes from 191.36 to 154.52 during epochs 1 and 10, indicating consistent and monotonic optimization of the ELBO. This persistent decline signifies that the parameters of both the encoder and decoder converge steadily without any training instability.

The reconstruction loss demonstrates the most substantial enhancement, decreasing from 185.52 to 148.59. This verifies that the decoder progressively apprehends the fundamental structure of MNIST digits. The decoder swiftly acquires broad structural information in the initial epochs, subsequently refining more intricate pixel-level details. The proximity of training and test reconstruction losses (148.59 vs. 148.92) further suggests negligible overfitting.

The KL divergence rises from 5.84 to 5.92 throughout the training duration. Despite the absolute quantity being minor in comparison to the reconstruction term, the incremental rise is theoretically noteworthy: it indicates the encoder's increasing alignment between the estimated posterior and the standard normal prior. This behavior signifies that the model prevents posterior collapse and preserves significant latent information.

The results from the test set corroborate these observations. The total loss during testing (154.80) strongly aligns with the final training loss, further substantiating robust generalization. The KL divergence on the test set (5.88) corresponds with that of the training set, indicating consistent latent behavior across unobserved data.

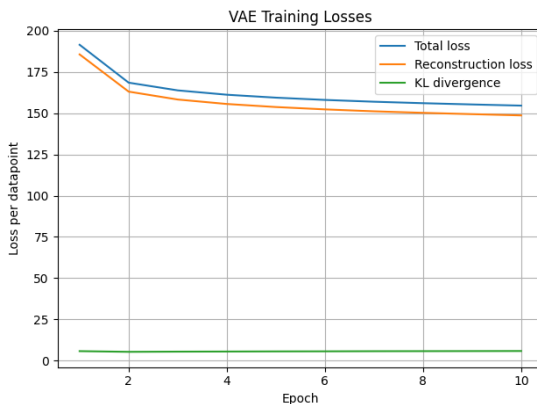


Figure 1: Training curves illustrate a reduction or stabilization in total loss, reconstruction loss, and KL divergence over 10 epochs.

Table 1. Training Loss Components per Epoch

| Epoch | Total Loss | Reconstruction Loss | KL Divergence |
|-------|------------|---------------------|---------------|
| 1 | 191.3637 | 185.5242 | 5.8395 |
| 2 | 168.4115 | 162.9912 | 5.4203 |
| 3 | 163.7463 | 158.2058 | 5.5406 |
| 4 | 161.1101 | 155.5063 | 5.6038 |
| 5 | 159.3406 | 153.6565 | 5.684 |
| 6 | 157.9629 | 152.2359 | 5.727 |
| 7 | 156.8715 | 151.0691 | 5.8024 |
| 8 | 155.989 | 150.1512 | 5.8378 |
| 9 | 155.2216 | 149.3451 | 5.8765 |
| 10 | 154.5172 | 148.5941 | 5.9231 |

6.2 Interpretation of Reconstruction

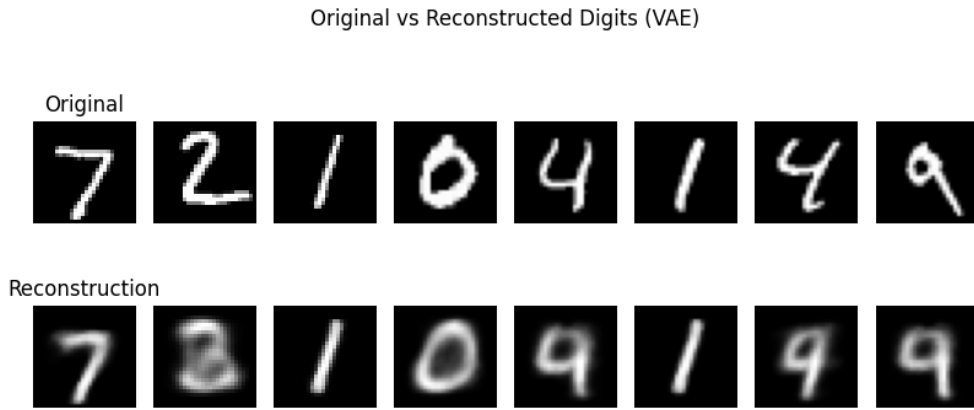


Figure 2: Original MNIST digits (top row) and their matching VAE reconstructions (bottom row). The model maintains digit identity while refining intricate details.

Figure 2 displays original MNIST digits in conjunction with their reconstructions. The model consistently maintains global structure and digit identification; nevertheless, intricate features like stroke width and edges seem somewhat softened. The smoothing effect is typical of VAEs, resulting from the pixel-wise independence assumption inherent in binary cross-entropy and the Gaussian likelihood interpretation. Notwithstanding these constraints, the reconstructions illustrate that the acquired latent representation preserves the fundamental information required to replicate the input data.

6.3 Interpretation of Latent Space

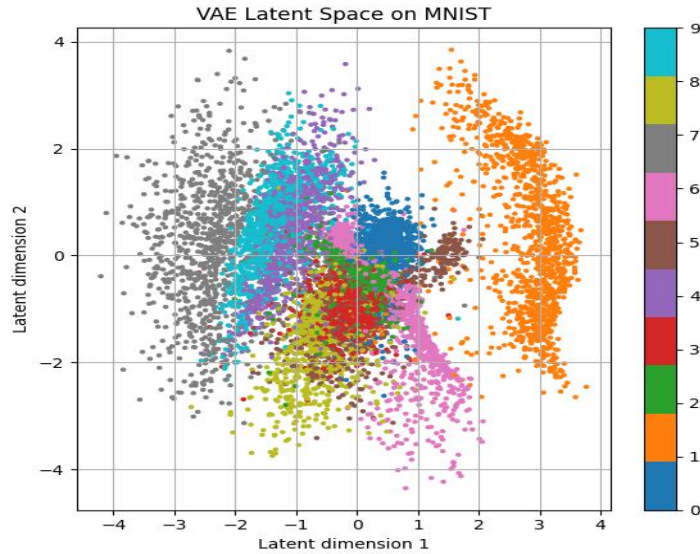


Figure 3 Two-dimensional latent space of MNIST encoded by the Variational Autoencoder. Points are categorized by digit class, exhibiting discrete and continuous clusters.

The two-dimensional latent space visualization in Figure 3 demonstrates evident clustering behavior, with digits occupying discrete yet partially overlapping regions. This verifies that the encoder allocates semantically like digits to adjacent regions of the latent manifold. For instance, numerals with analogous forms (such as 3 and 5) are positioned in proximity to one another. The continuity of the embedding demonstrates the VAE's ability to learn smooth mappings from image space to latent space, a crucial requirement for significant interpolation and regulated generation.

6.4 Generative Efficacy

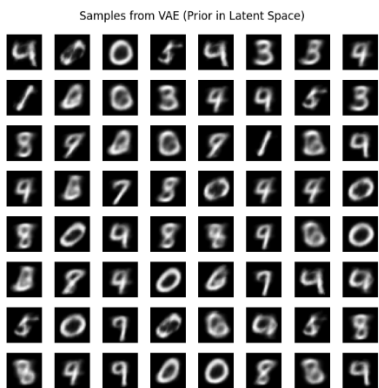


Figure 4: Digits produced by decoding random latent vectors sampled from the standard normal distribution. The majority of samples resemble authentic MNIST digits.

Random previous samples translated into pictures (Figure 4) exhibit cohesive digit-like formations. Although certain examples display ambiguity or uneven strokes, the majority of generated images conform to the manifold of valid MNIST digits. This suggests that the acquired posterior distribution is adequately consistent with the prior to provide credible generative sampling.

7. Conclusion

This course illustrated the integration of probabilistic modeling and deep neural networks with Variational Autoencoders to acquire structured latent representations and produce novel data. The model demonstrated persistent ELBO optimization, enhanced reconstruction accuracy, and well-defined latent clusters that represent semantic links among digits through testing on the MNIST dataset. The VAE effectively produced coherent digit samples, validating the correspondence between the learnt posterior and the Gaussian prior. Despite certain reconstructions and samples exhibiting blurring—a recognized disadvantage of VAEs—overall performance suggests that the model effectively captures fundamental data structure while preserving a smooth, interpretable latent geometry. These findings underscore the VAE's utility as both a generative model and a dimensionality reduction instrument. The course demonstrates how loss decomposition, latent space visualization, and generative sampling yield significant insights into model behavior, enhancing comprehension of probabilistic representation learning.

References

- Kingma, D. P., & Welling, M. (2014). *Auto-Encoding Variational Bayes*. International Conference on Learning Representations (ICLR).
<https://arxiv.org/abs/1312.6114>
- Rezende, D. J., Mohamed, S., & Wierstra, D. (2014). *Stochastic Backpropagation and Approximate Inference in Deep Generative Models*. Proceedings of the 31st International Conference on Machine Learning (ICML).
<https://arxiv.org/abs/1401.4082>
- Doersch, C. (2016). *Tutorial on Variational Autoencoders*.
<https://arxiv.org/abs/1606.05908>
- Goodfellow, I., Bengio, Y., & Courville, A. (2016). *Deep Learning*. MIT Press. (Chapter 20: Deep Generative Models)
- Murphy, K. P. (2022). *Probabilistic Machine Learning: Advanced Topics*. MIT Press.

PyTorch Documentation. *VAE Examples and Implementation Notes.*

<https://pytorch.org/tutorials>